PREPRINT NO. 933 (B-7)

OPTIMUM HORN MOUTH SIZE

by
D. B. Keele, Jr.
Electro-Voice, Inc.
Buchanan, Michigan

PRESENTED AT THE
46th CONVENTION
SEPTEMBER 10-13, 1973

AN AUDIO ENGINEERING SOCIETY PREPRINT

Convention Price . . . . . . $ .50
By Mail to Members . . . . $ .75
By Mail to Non-Members . . $1.00

This preprint has been reproduced from the author's advance manuscript, without editing or corrections. For this reason there may be changes should this paper be published in the Audio Engineering Society Journal.

Additional preprints may be obtained by sending request and remittance to the Audio Engineering Society Room 929, 60 East 42nd Street, New York, N. Y. 10017.

© Copyright 1973 by the Audio Engineering Society
All rights reserved

OPTIMUM HORN MOUTH SIZE

By D. B. Keele, Jr.

ELECTRO-VOICE, Inc., Buchanan, Michigan 49107

Loudspeaker exponential horn computer model studies indicate that there is an optimum mouth size for a horn of specific cutoff to minimize mouth reflections. Evaluation of the reflection coefficient at the horn's mouth reveals how large the mouth must be to optimally radiate into different size solid angles.

INTRODUCTION

This paper describes some rather surprising results encountered while checking the simulations of a digital computer model of the loudspeaker horn. Conventional exponential horn theory states that for maximum efficiency and minimum mouth reflections the finite horn's mouth size must be equal to <u>or larger than</u> a certain fraction of the wavelength at the cutoff frequency (usually assumed to be that size where the horn's mouth circumference is equal to the cutoff frequency wavelength) [1, p. 268], [2, p. 453], [3, p. 366], [4, p. 278], [5, p. 242]. The implied assumption is that you can approach arbitrarily close to the ideal infinite horn operation just by making the finite horn's mouth (and length) larger and larger. The theoretical research described in this paper will show that this assumption is false and that there is a definite optimum mouth size for minimization of internal reflections from the horn's mouth. The optimum mouth size is found to be strongly dependent on the solid angle into which the horn is radiating.

A DISCOVERY

To facilitate design of loudspeaker horns a generalized loudspeaker horn computer model was developed. The model simulates both the electrical and acoustical operation of the horn with emphasis on the horn's activity from the standpoint of the driver (the model will not predict directional characteristics). A future paper will describe the details of this model.

In an attempt to verify the predictions of the acoustic portion of the model, a pure exponential horn was simulated. A plot of the normalized acoustic throat impedance versus frequency was generated with the mouth of the model terminated in the standard half space (2π steradian, rigid flat circular piston model in an infinite flat baffle) radiation load [6, p. 92] . A series of runs were computed with constant flare cutoff frequency of 100 Hz and throat diameter of one inch while the mouth diameter and length were stepped through several different values. These particular numbers were chosen so that the model's output could be compared with the operation of the theoretical single parameter wave mathematical model as shown in the now classic work by Olson [6, p. 111, Fig. 5.10] (reproduced here as Fig. 1).

An examination of Fig. 1 seems to indicate that in general the throat impedance ripple magnitude decreases as the mouth is made larger. The reverse traveling waves generated by the mouth reflections generate the deviations in throat impedance above and below the infinite throat impedance characteristic. For small mouth diameters ($k_C\, a_M \ll 1$ where $k_C = 2\pi/\lambda$ at cutoff and a_M = mouth radius) the horn acts essentially like a resonant tube.

The computer model's output agreed fairly well with Olson's depicted data up to and including mouth diameters of 30 inches ($k_C\, a_M = 0.7$ at cutoff). The surprise came when the plot was continued for large mouths ($k_C\, a_M > 1$) where the ripple was seen to increase quite sharply and attain a limit value for extremely large mouths ($k_C\, a_M > 10$).

At first the author thought his computer model was at fault but after much checking and head scratching this was not found to be the case. A direct programming of Olson's eq. 5.80 [6, p. 108] (reproduced here in somewhat different form as eq. 8), the expression relating the mouth and throat impedances of the finite exponential horn in terms of the length and flare constant, revealed the same ripple magnitude increase for large mouths (see Fig. 2). Thus it was found that in reality no fault existed in the author's model but that single parameter wave horn theory also predicts a type of mouth-air mismatch which occurs for large mouth sizes.

The author in the remaining sections of this paper will attempt to explain this phenomenon using transmission line analogies, and then apply the tools developed to a determination of how large a horn must be for radiation into a specific environment.

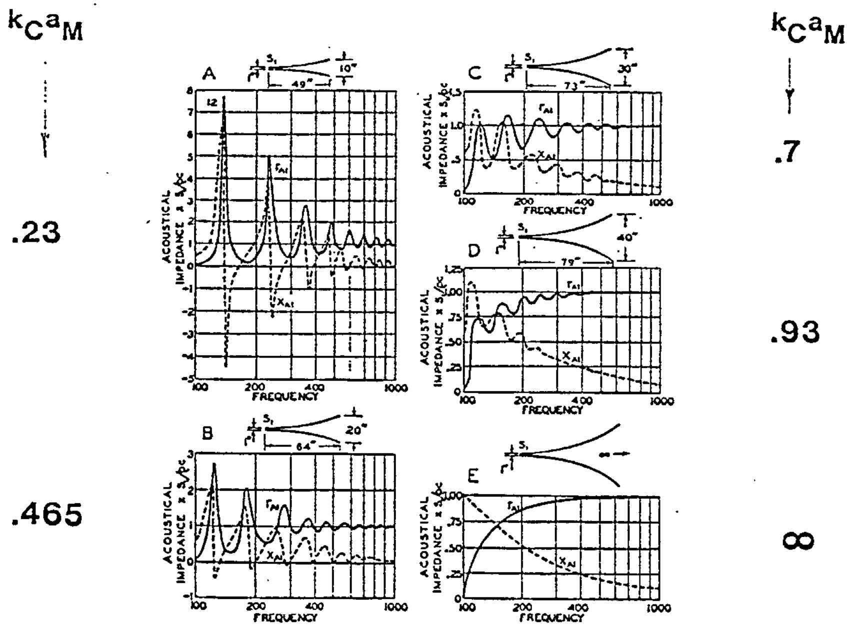

FIG. 5.10. The throat acoustical resistance and acoustical reactance frequency characteristics of a group of exponential horns, with a flare cutoff of 100 cycles and a throat diameter of 1 inch, as a function of the mouth diameter. S_1 = the throat diameter in square centimeters. r_{A1} = acoustical resistance. x_{A1} = acoustical reactance. Note: The characteristics shown are the throat acoustical resistance or acoustical reactance multiplied by S_1 and divided by ρc.

Fig. 1. Reproduction of Olson's [6, p. 11] classic exponential horn data illustrating how the throat acoustic impedance varies as the horn mouth size is changed. (Courtesy of Olson and D. Van Nostrand Co., Inc.).

SOME THEORY

The Acoustic Transmission Line --

The well known equation which gives the variation of area as a function of axial distance for the infinite exponential horn appears as [6, p. 103] :

$$S = S_1 e^{mX} \tag{1}$$

where S_1 = throat area (= S (0)),

X = axial distance from throat,

m = flare constant $(= 4\pi f_C/C)$,

f_C = horn cutoff frequency, and

C = speed of sound in air.

A solution of the one-parameter wave equation inside a duct whose area varies as (1) yields a set of equations which gives the real and imaginary components of the acoustical impedance at any point X where the area is S [6, p. 103] :

$$r_A = \frac{\rho_o C}{S} \sqrt{1 - \frac{m^2}{4 k^2}} \quad \text{, and} \tag{2}$$

$$A = \frac{\rho_o C}{S} \frac{m}{2k} \tag{3}$$

Where ρ_o = density of air.

Below cutoff $(f < \frac{mC}{4\pi})$ the horn's impedance is purely imaginary with magnitude:

$$x_A = \frac{\rho_o C}{S} \left(\frac{m}{2k} - \sqrt{1 - \frac{m^2}{4k^2}} \right) \tag{4}$$

Equations (2), (3) and (4) may be simplified by substitution of the normalized variables:

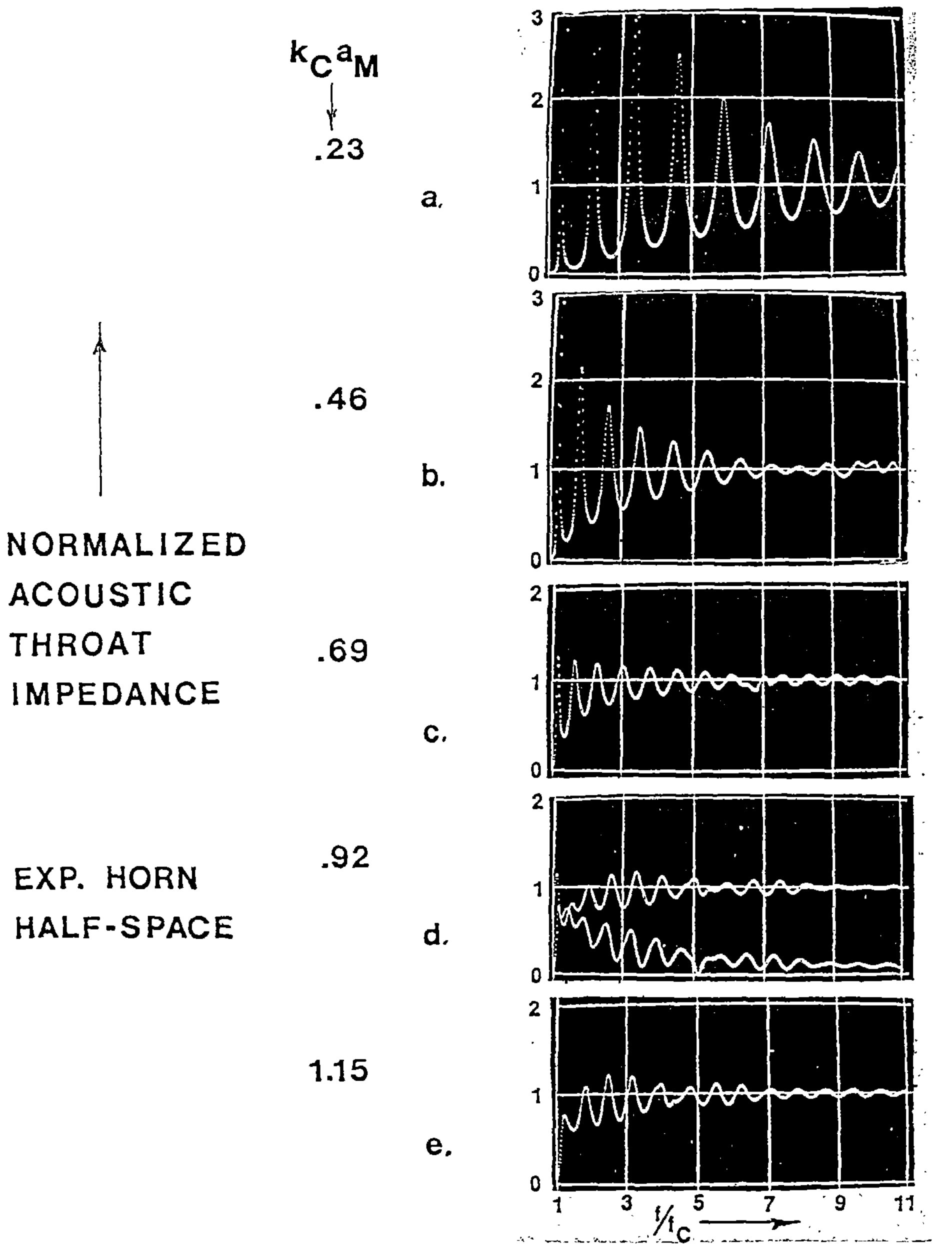

Fig. 2. Exact solution of eq. (8) by digital computer as plotted on C.R.T. display showing the variation of horn throat impedance as the horn mouth size is varied. The horn parameters match those of Olson (Fig. 1). Note linear impedance and frequency scales. The real component of throat impedance is

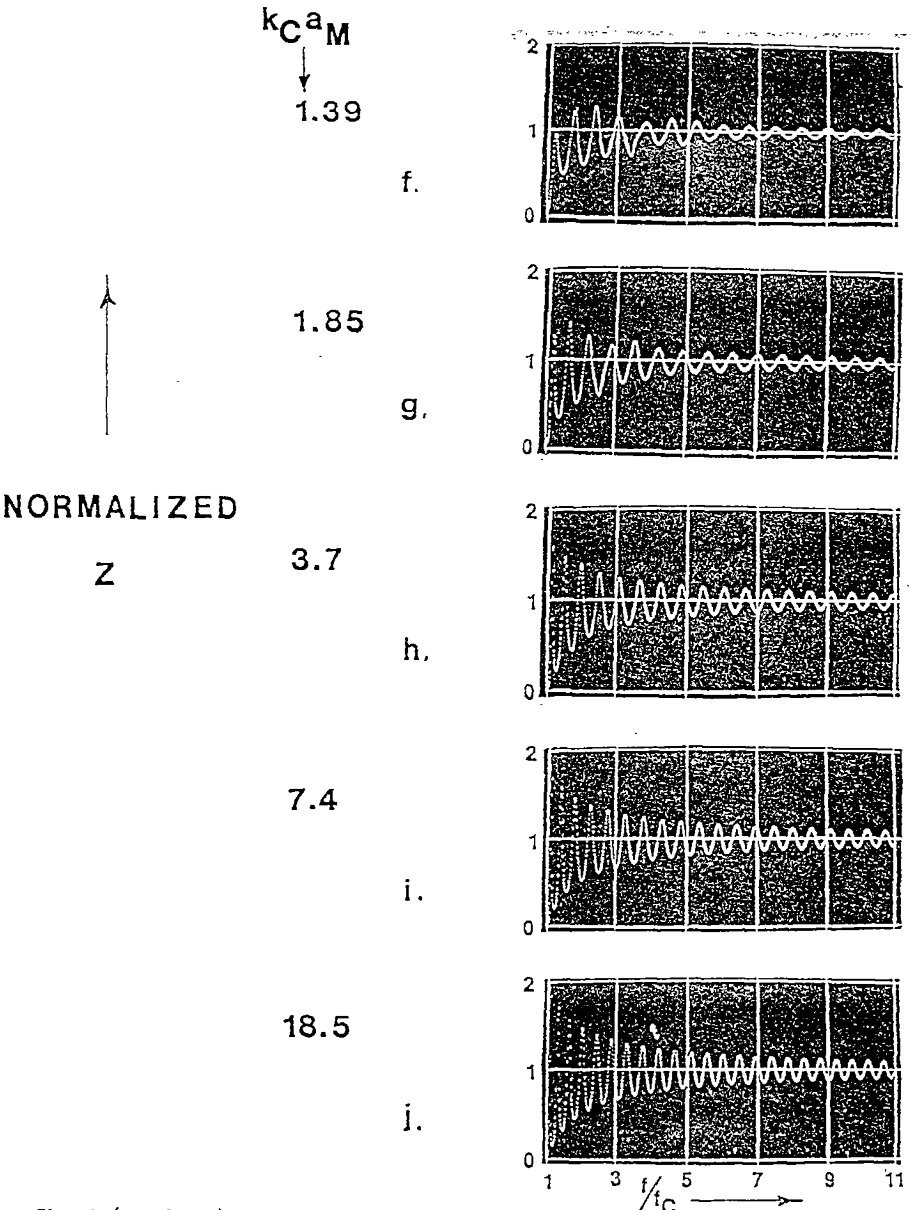

Fig. 2 (continued)
plotted in every case except for d. where both real and imaginary components are shown. The averaged R.M.S. ripple as compared to the infinite throat impedance characteristic (Fig. 3) is as follows (averaged from f_C to 11 f_C): a. 0.832, b. 0.279, c. 0.112, d. 0.072, e. 0.089, f. 0.111, g. 0.137, h. 0.161, i. 0.176, and j. 0.188.

$u = f/f_c = 2k/m$, $R_A = r_A S/(\rho_o C)$, and $X_A = x_A S/(\rho_o C)$

yielding at or above cutoff:

$$R_A = \sqrt{1 - 1/u^2} \text{ , and} \tag{5}$$

$$X_A = 1/u. \tag{6}$$

The corresponding below cutoff equation is:

$$X_A = 1/u - \sqrt{1/u^2 - 1} . \tag{7}$$

Notice that equations (5), (6), and (7) which give the normalized acoustic impedance at any point along the axis of an infinite exponential horn are position independent. In terms of the electric transmission line analogy these equations can be thought of as describing the so-called characteristic impedance of the horn transmission line. The behavior of these equations is illustrated in Fig. 3.

The equation which relates the normalized mouth and throat impedances for the finite exponential horn above cutoff appears as [6, p. 108, eq. 5.80] :

$$Z_T = \frac{Z_M \cos(bl + \emptyset) + j \sin(bl)}{\cos(bl - \emptyset) + j Z_M \sin(bl)} \tag{8}$$

where Z_M = normalized acoustic impedance terminating the mouth,

Z_T = normalized acoustic impedance appearing at throat,

l = length of horn,

$\theta = \tan^{-1}(1/\sqrt{u^2 - 1})$,

$b = m\sqrt{u^2 - 1}/2$, and

$\mu = f/f_c$.

The Load --

The nature of the radiation load that terminates the horn transmission line depends on the solid angle into which the horn radiates. Three specific cases will be considered in this paper: full space (4π steradians), half space (2π steradians), and fractional space ($\Psi < \pi$ steradians). The respective loads used to model these angles are described as follows.

1. Full Space

   The impedance functions of a rigid circular piston mounted in the end of a very long tube as originally derived by [7, p. 383] and described by [6, p. 97], and [1, p. 123].

2. Half Space

   The impedance functions of the rigid circular piston mounted in a flat baffle of infinite extent as described in [6, p. 92] and [1, p. 118] (Fig. 4).

3. Fractional Space

   The termination load presented is that of the throat of an infinite conical horn whose conical solid angle equals the radiation angle in question. The real and imaginary components of the normalized acoustic impedance at the throat of a conical horn are given by [6, p. 103]:

$$R_A = \frac{(k\,X_1)^2}{1 + (k\,X_1)^2}, \text{ and} \tag{9}$$

$$X_A = \frac{k\,X_1}{1 + (k\,X_1)^2}, \tag{10}$$

where X_1 = distance of throat from cone apex $X = 0$,

$k = 2\pi / \lambda$, and

λ = wavelength.

For a specific conical horn of throat radius a_T and half angle θ, X_1, is given by [8, p. 271]:

$$X_1 = a_T / \sin\theta. \tag{11}$$

A simple integration shows the relation between the conical solid angle Ψ and the cone's half angle θ:

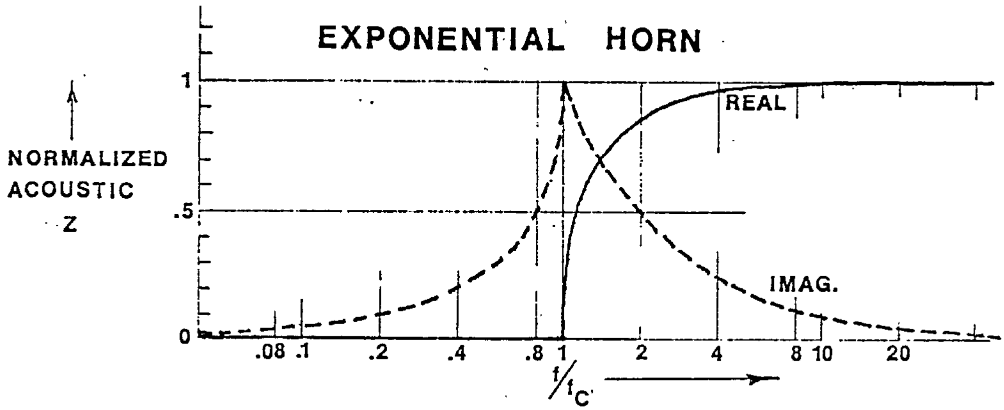

Fig. 3. The characteristic acoustic transmission line impedance of the exponential horn as computed from eqs. (5), (6), and (7).

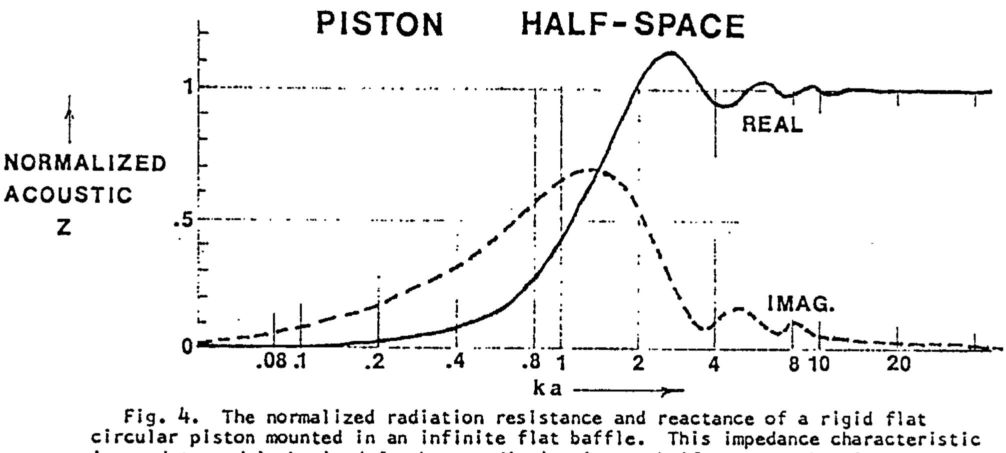

Fig. 4. The normalized radiation resistance and reactance of a rigid flat circular piston mounted in an infinite flat baffle. This impedance characteristic is used to model the load for horn radiation into a half-space. The piston radius is "a" while k = w/c = 2π/λ .

$$\Psi = 2\pi\ (1 - \cos\theta) \tag{12}$$

Only the half space load for the exponential horn will be dealt with in any detail in this paper.

The System --

The system composed of the horn transmission line and its terminating radiation load impedance can be analyzed in much the same way as any other electrical transmission line. If a line of characteristic impedance Z_0 is connected to a load of impedance Z_L a voltage wave (or pressure wave) reflection coefficient ρ may be defined [9, p.19]:

$$\rho = \frac{Z_L - Z_0}{Z_L + Z_0} \tag{13}$$

If both the line and load impedances are complex the reflection coefficient is of course also complex. For this specific case the magnitude of ρ is a good figure of merit for minimization of reflections. It must be noted that for minimum reflections ($|\rho| \ll 1$), the real parts of the line and load Z and the complex parts of the line and load Z must be in equality independent of each other.

APPLICATION

A fairly complete analysis of the exponential horn radiating into a half space environment will be done in this section.

The characteristic line impedance of the exponential horn was given previously in (5), (6), and (7) and illustrated in Fig. 3. The half space radiation load seen by the horn (modeled by a rigid flat piston radiating into a half space) is shown in Fig. 4 and given by [6, p. 92, eq. 5.10]

A thoughtful observation and comparison of Figs. 3 and 4, keeping in mind eq. (13), reveals a rough correspondence between the real and imaginary parts of the impedance functions only when the mouth diameter is such that $k\ a_M \approx 1$ at the horn's cutoff frequency. Different size mouth diameters reflect in relative shifts in the curves along the frequency axis as shown in Fig. 5. The mismatch for small mouth diameters is self evident. For large mouth diameters the mismatch is caused by the load impedance being essentially real and unity while the horn's line impedance is highly complex particularly over the range f_C to $4\ f_C$.

SMALL MOUTH

$k_C a_M = 0.1$

OPTIMUM

$k_C a_M = 1$

LARGE MOUTH

$k_C a_M = 10$

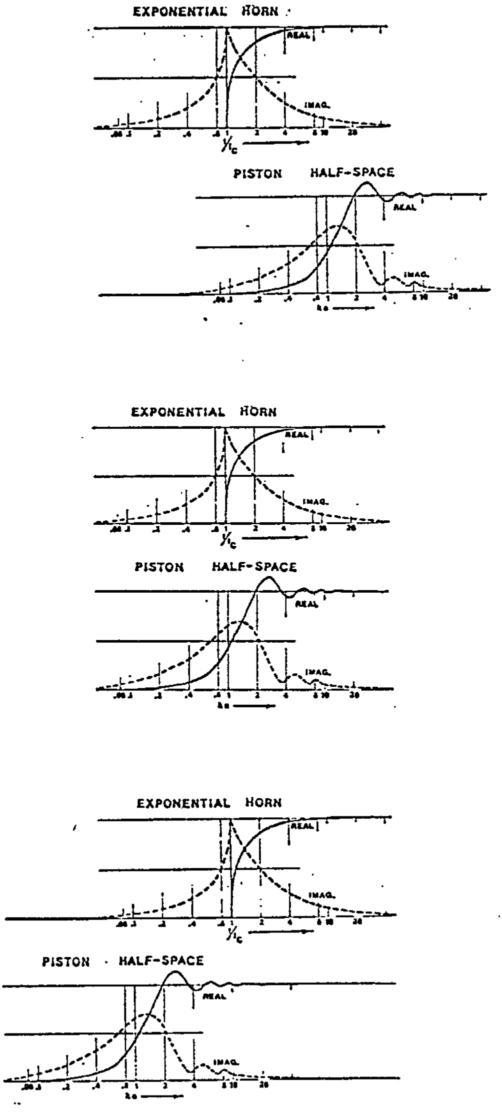

Fig. 5. Illustration of the effects of varying mouth size on the horn line impedance--load impedance match. Rough correspondence occurs between both the real and imaginary components only when ka is about one at the horn's cutoff frequency.

To illustrate the behavior of the magnitude of the reflection coefficient as it applies to the exponential horn radiating into a half space, the appropriate equations were programmed on the computer and the results shown here in Fig. 6. Indeed these curves show that a rough minimum occurs in $|\rho|$ at about $k_C\, a_M = 1$.

To determine the optimum mouth sizes a program was written which yielded the root mean square (RMS) value of the magnitude of the reflection coefficient ($|\rho|_{RMS}$) averaged over specific frequency intervals. Three frequency bands were chosen covering f_C to $2\, f_C$, $2\, f_C$ to $10\, f_C$, and f_C to $10\, f_C$. The results of these computations are shown in Fig. 7.

The values plotted clearly show the minimums in reflection for certain values of $k_C\, a_M$. For minimization of reflections in the interval from f_C to $2\, f_C$ the mouth must be somewhat larger than if the frequency range of interest is only over $2\, f_C$ to $10\, f_C$. For the interval of f_C to $10\, f_C$ the optimum mouth size is found to be $k_C\, a_M = 0.935$. Fig. 8 shows a plot of the throat impedance and the reflection coefficient magnitude for this specific case. Note the close correspondence between the ripple magnitude and the value of the reflection coefficient. The ripple magnitude is seen to increase and decrease in cycles as the frequency is increased.

The corresponding plot of $|\rho|_{RMS}$ for radiation into full and fractional spaces is shown in Figs. 9 and 10. The fractional space illustration is shown as a function of $k_C\, a_M / \sin\theta$ where θ and the solid angle Ψ are related by eq. (12).

RESULTS

The results of this paper's study are tabulated in Table I which shows the optimized values of $k_C\, a_M$, for the given solid angles evaluated, along with the frequency ranges over which the reflection coefficient was minimized.

It must be pointed out to the reader that the accuracy of the data derived in this paper depends on how well the assumed radiation load model agrees with the actual physical conditions at the mouth of the horn. The constant phase wavefront at horn's mouth is neither planer nor spherical and in addition changes shape with frequency because of mouth reflections.

McLachlan (1934) [10, ch. X] in an exhaustive but not so well read study of exponential horns realized the importance of matching both the real and imaginary components of horn and load impedance and determined that the optimum mouth size for half space radiation (using a pulsating hemisphere as a load model) occurred somewhere in the range $1 < k_C\, a_M < 2$.

An interesting observation of Fig. 6a is that the reflection coefficient for frequencies much less than cutoff reaches a limiting value which depends highly on $k_C\, a_M$. A $k_C\, a_M$ value of roughly one appears to minimize the reflections over the whole operating range including those frequencies at and below cutoff. A none unity value for the reflection coefficient at and below cutoff indicates that power can be transmitted by the horn in this region (which is what everybody knew all along anyway).

CONCLUSIONS

This research has shown that one parameter wave exponential horn theory predicts optimum mouth size which minimizes internal reflections from the horn's ch. The size of the mouth is found to depend on the cutoff frequency of the horn and the solid angle of horn radiation.

ACKNOWLEDGEMENT

The author wishes to thank his colleagues at Electro-Voice, John Gilliom and Ray Newman, for comments and criticisms of this work. Appreciation is extended to Dr. William J. Strong of the physics department at Brigham Young University for doing an independent confirmation of the described phenomena resulting in the work displayed in Fig. 2 of this paper.

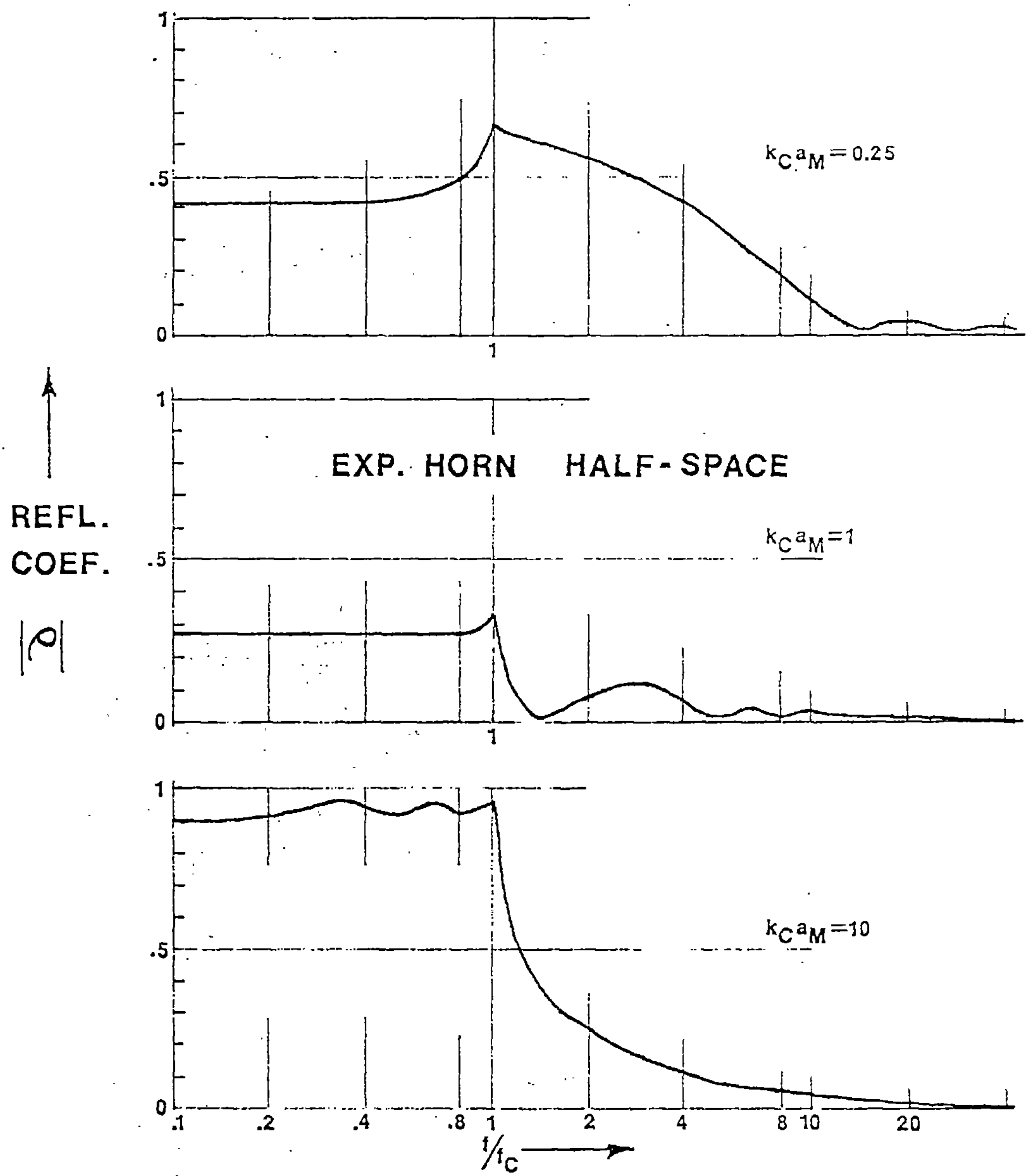

Fig. 6a. Plot of the magnitude of the reflection coefficient for exponential horn radiation into a half-space for the indicated values of $k_C a_M$ over the frequency range 0.1 f_C to 40 f_C.

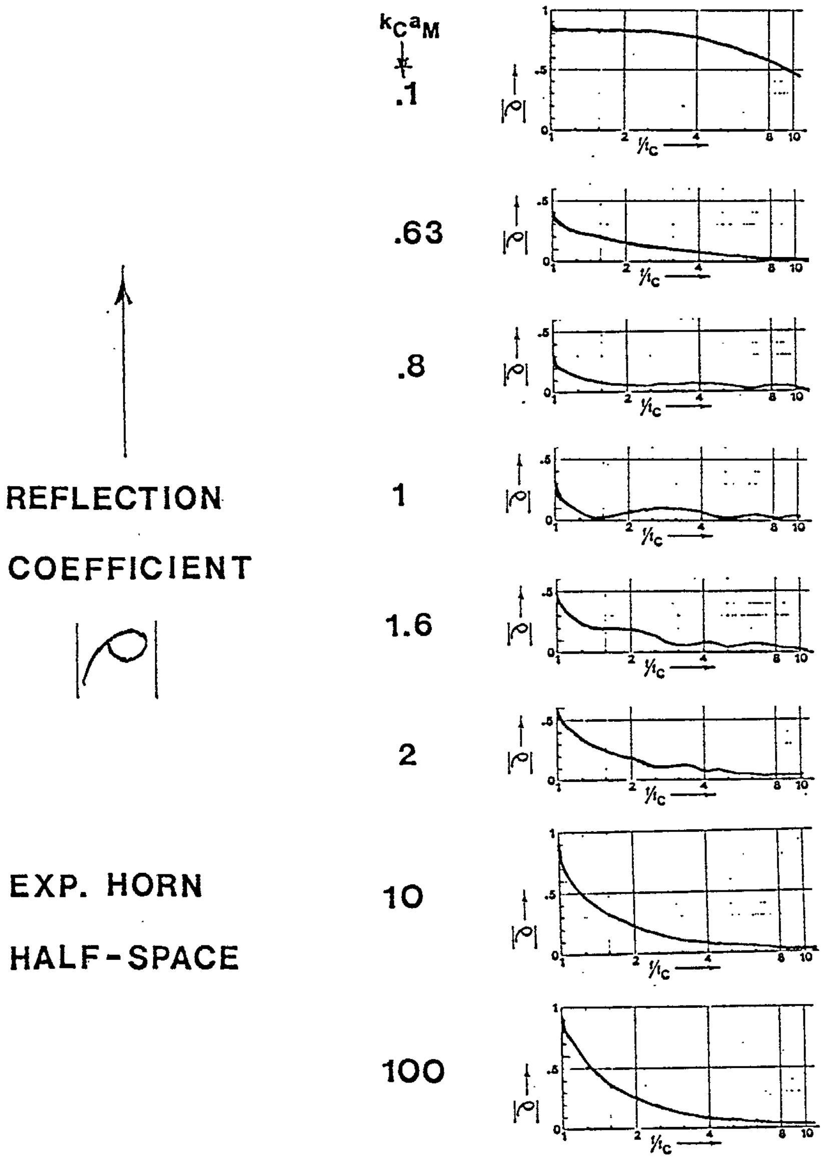

Fig. 6b. Plot of the magnitude of the reflection coefficient for exponential horn radiation into a half-space for the indicated values of $k_C\ a_M$ over the frequency range f_C to 10 f_C. A definite rough minimum in $|\rho|$ occurs at $k_C\ a_M = 1$.

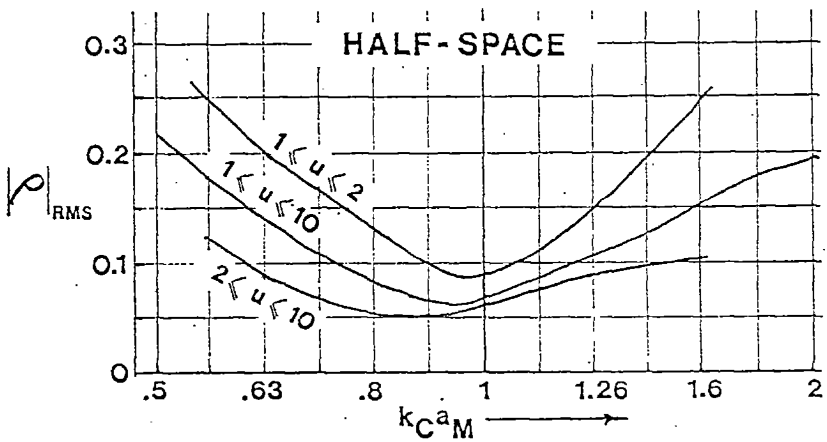

Fig. 7. The root mean square value of the magnitude of the reflection coefficient integrated over the indicated frequency ranges ($u = f/f_C$) for exponential horn radiation into a half-space. The minimums occur at: 0.975 for $1 \leq u \leq 2$, 0.935 for $1 \leq u \leq 10$, and 0.825 for $2 \leq u \leq 10$.

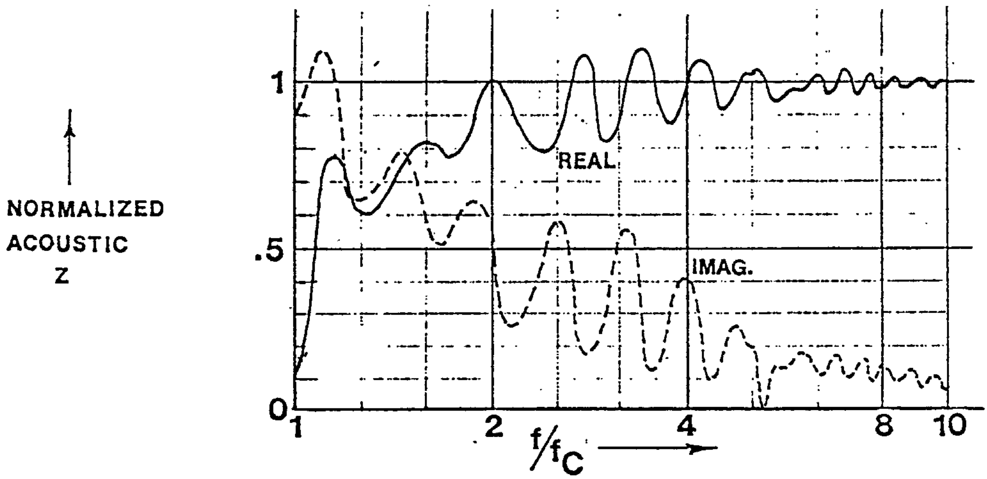

EXP. HORN HALF-SPACE

$k_C a_M = .935$

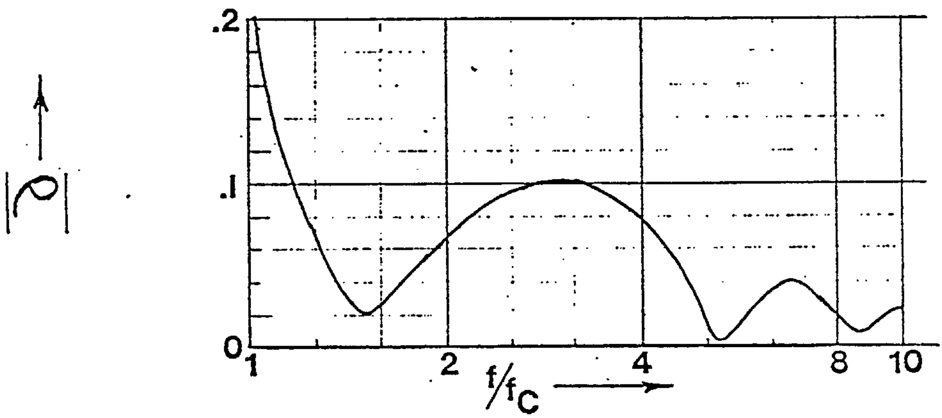

Fig. 8. Comparison of the throat impedance and reflection coefficient magnitudes for the exponential horn radiating into a half-space for the specific value of k_C a_M which minimizes $|\rho|_{RMS}$ over the interval f_C to 10 f_C. Compare this computer generated plot of throat Z with Fig. 1 for the 40 inch diameter mouth.

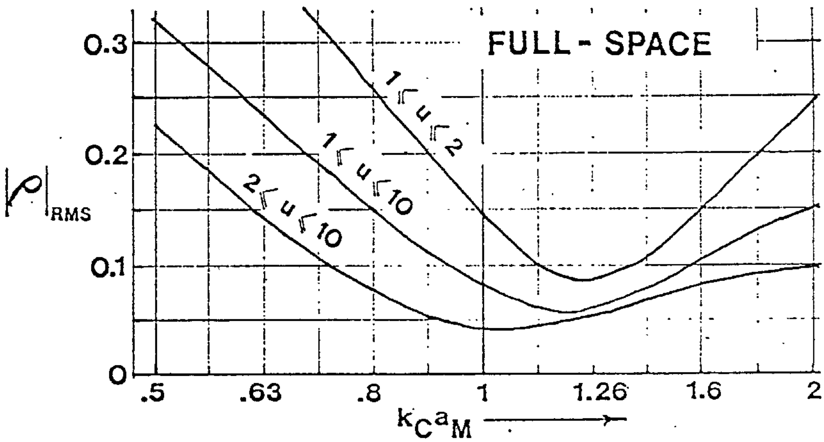

Fig. 9. The root mean square value of the magnitude of the reflection coefficient integrated over the indicated frequency ranges ($u = f/f_C$) for exponential horn radiation into a full-space. The minimums occur at: 1.249 for $1 \leq u \leq 2$, 1.199 for $1 \leq u \leq 10$, and 1.024 for $2 \leq u \leq 10$.

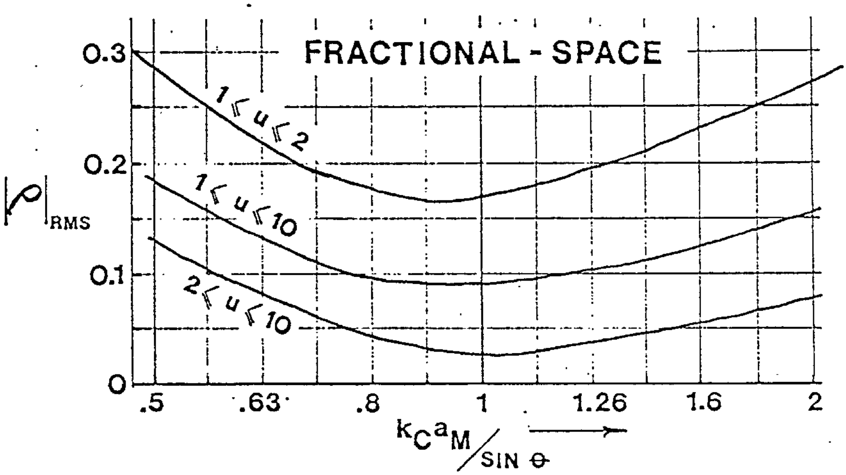

Fig. 10. The root mean square value of the magnitude of the reflection coefficient integrated over the indicated frequency ranges ($u = f/f_C$) for exponential horn radiation into fractional-space ($\psi \leq \pi$). The minimums occur at: 0.928 for $1 \leq u \leq 2$, 0.954 for $1 \leq u \leq 10$, and 1.00 for $2 \leq u \leq 10$.

TABLE I OPTIMIZED k_C a_M

Fractional-Space $0 < \Psi < \pi$	Half-Space $\Psi = 2\pi$	Full-Space $\Psi = 4\pi$	Optimized Freq. Range
$0.954 \times \sin\theta$	0.935	1.199	f_C to 10 f_C
$0.928 \times \sin\theta$	0.975	1.249	f_C to 2 f_C
$1.00 \times \sin\theta$	0.825	1.024	2 f_C to 10 f_C

where:

Ψ = solid angle of radiation ($= 2\pi(1 - \cos\theta)$)

θ = half angle of cone with solid angle Ψ

$k_C = 2\pi/\lambda_C = 2\pi f_C/C$

a_M = horn mouth radius

REFERENCES

[1] L.L. Beranek, Acoustics (McGraw-Hill, New York, 1954).

[2] A. Wood, Acoustics (Dover Publications, Inc., New York, 1966).

[3] J.L. Bernstein, Audio Systems (John Wiley and Sons, Inc., New York, 1966).

[4] L.E. Kinsler, A.R. Frey, Fundamentals of Acoustics (John Wiley and Sons, Inc., New York 1962).

[5] A.B. Cohen, HI-FI Loudspeakers and Enclosures (Hayden Book Co., Inc., New York 1968).

[6] H.F. Olson, Acoustical Engineering (D. Van Nostrand Co., Inc., New York 1960).

[7] H. Levine, J. Schwinger, "On the Radiation of Sound from an Unflanged Circular Pipe," Physical Review, vol. 73, no. 4, p. 383 (Feb. 1948).

[8] P.M. Morse, Vibration and Sound (McGraw-Hill Book Company, Inc., 1948).

[9] R.G. Brown, Lines, Waves, and Antennas (The Ronald Press Co., New York 1961).

[10] N.W. McLachlan, Loudspeakers (Dover Publications, Inc., New York, reprinted 1960).